LIGO-P070055-00-Z

Journal : Mechanical Systems and Signal Processing

Title

Active control and sensor noise filtering duality, experimental application to advanced LIGO suspensions

Authors

Laurent RUET, Massachusetts Institute of Technology

Richard Mittleman, Massachusetts Institute of Technology

Luc Gaudiller, LAboratoire de Mécanique des COntacts et des Structures

Johan Der Hagopian, LAboratoire de Mécanique des COntacts et des Structures

David Ottaway, Massachusetts Institute of Technology

1 ABSTRACT

Active damping is often used in high precision vibration isolation. In systems where extreme levels of isolation are required, the sensors used in active damping can inject noise that can significantly degrade the performance of the system. In this paper, an independent modal control combined with a state estimator is designed to minimize the effect of sensor noise re-injection while maintaining effective damping control. Tools are developed to balance damping and sensor noise injection minimization. This method is applied to the last stage of an Advanced LIGO seismic isolation system which is a multi-stage pendulum system. A comparison between a classic filtering approach and the modal control and estimation method is shown. These results are experimentally validated using optical techniques to measure the distance between two isolated tests masses. Displacement noise of order less than an angstrom can easily be measured using this technique.

Keywords :
Active control
Vibration
Sensor noise
Filtering
LIGO

2 INTRODUCTION

The detection of gravitational waves is one of the biggest challenges for modern physics and mechanical engineering. Gravitational waves are generated by the acceleration of massive objects in space and were predicted by Einstein [1] in 1916. The detection of such waves is important for several reasons. First it will allow some of the predictions of General Relativity to be tested. Secondly, it will provide new information on astrophysical events in the universe, for example the collapse of stars or interactions of black holes. The current detectors [2][3][4][5] attempt to detect these waves using optical interferometry to measure the strain they produce as they pass through the earth. The strain of this signal when it reaches the earth is extremely small, and to attain such an extraordinary sensitivity, it is necessary to design a system to isolate the instruments from the ground's vibrations.

Vibrations isolation is a very common problem in the engineering field and various approaches can be used. Traditionally, passive control systems [6] that don't require an external power

source are used to attenuate or cancel mechanical vibrations. Two different kind of passive systems can be found: Passive dampers [7] are used to dissipate the energy of the system through localized devices such as rubber, oil or friction systems. Passive isolators [8][9] are used to isolate a system from an input noise. In these systems, a flexible isolation system is introduced between the input noise and the structure. By tuning this flexibility, the transmitted vibrations can be reduced or eliminated. These isolators are very often limited to high frequencies.

In the last few decades, advances in digital signal processing, sensors and actuators technology have prompted interest in active vibration control [10][11]. These systems can be defined as systems which require external power for operation: sensors measure the motion of the structure, the measurements are then processed and actuators apply a response to counter-act the displacement. Depending on the location of the actuators and the software that pilots them; active control can either be used for damping purposes [12] or vibration isolation [13][14]. The advantages of active control are the flexibility and the ability to perform at lower frequencies. However, active control is expensive and as will be shown in this article, sensors and actuators can generate additional noise in the system.

Very often, a hybrid passive/active system [15][16] can be used. It provides the advantages of the passive isolation with the flexibility of the active vibration isolation. Many example of hybrid vibrations isolation can be found in transportation systems [17] or building seismic protection [18]. It is also used for the gravitational waves detectors to isolate the instruments from the ground motion.

The proposed Advanced American Gravitational Waves detector, named Advanced LIGO [19], will use three stages of seismic isolation systems [20][21]. The last stage is a pendulum that utilizes passive isolation to reduce the high frequencies noise. The last mass of this pendulum is the test mass whose position is sensed by the interferometer. At 10 Hz, it is anticipated that the combination of the three stages will reduce the displacement noise of the test mass of the pendulum to about $10^{-19} m/\sqrt{Hz}$.

In order for the interferometer to function correctly, the pendulum rigid-body resonances that have frequencies between 0 and 10Hz are damped using digital active control loops. However, at the required sensitivity, the effect of sensor noise is not negligible. In advanced LIGO, the sensor noise [22] is expected to be up to a 100 times higher than the seismic noise at the point where the pendulum attaches to the seismic isolation system. This sensor noise will be processed in the control loop and re-injected into the pendulum, adding undesired displacement noise at

frequencies above the resonances. Therefore, it is necessary to design a control loop that provides damping while minimizing the sensor noise re-injection.

Most active control systems in LIGO are designed using the measured frequency-response. It has the advantage of being wideband and doesn't require a model of the structure if accurate measurements can be achieved. The current damping loops for LIGO are using collocated feedback with IIR filters[23][24]. We will show that this method introduces extra sensor noise at high frequencies into the loop.

Several alternate methods have been studied to minimize this sensor noise re-injection. The first approach consisted of improving the sensors, S. Aston and C. Speake have worked to increase the sensitivity in the sensors by using interferometric techniques [25] This sensor has a lower noise floor, it is expensive and complex.

A less costly solution was studied by K. Strain [26]. He proposed using a combination of active and passive damping. In his method, the lowest modes are still controlled actively but the highest modes are damped using the eddy current effect. This solution reduces the sensor noise transmission but increases the coupling between the pendulum and its frame, which can lead to more noise at high frequencies.

More recently, an interesting technique has been developed by G. Losurdo and D. Passuello [27] for VIRGO. Their purely active loop is split into two loops using complementary filters; one is actuating on the real pendulum at low frequencies while the other one is acting on a virtual model of the pendulum at the high frequencies. The combination of both loops is identical to a classic feedback but in this case, the virtual model "absorbs" the re-injection of the high frequencies sensor noise. This idea is very promising but mismatches in the model remain to be studied and the filtering of the sensor noise is also limited. A reliable, non expensive solution remains to be found to minimize the sensor noise re-injection while providing the desired damping performance.

In this work, the sensor noise injection will be minimized by using advanced active control loop topologies. The new approach will take advantage of the knowledge of the Advanced LIGO pendulum's dynamics and won't require any additional hardware or cost. Independent Modal Control [28][29] will be used to damp each mode of the pendulum separately. One of the advantage of the IMC is that it gives more freedom to the designer. By controlling modes one by one, it is possible to identify which modes transmit more sensor noise. This modal control will be coupled with an observer [30] that can be used to reconstruct the states that we cannot measure. Commonly, observers[31] are designed so that their poles are much faster than the controller's to insure stability. In this work, The knowledge of the plant will be used to design a slower estimator [32] that filters the sensor noise.

The loop will then be tested on a working Advanced LIGO suspension to validate the models and simulations. The order of magnitude of the vibrations that need to be measured is smaller than a nanometer, in order to measure such a small displacement of the test mass, a laser beam resonating inside the optical cavity formed by two triple pendulums will be used [33][34]. A comparison of the model and the experiment is performed to check the validity of the simulations.

3 ADVANCED LIGO & SUSPENSIONS

3.1 GRAVITATIONAL WAVES

In spite of the extraordinarily small strain that can be expected on earth, several methods have been proposed to detect gravitational radiation. In more recent times, most research effort has been directed toward laser interferometric detectors, and at this time, several countries have commissioned detectors of this type.

A laser interferometer gravitational wave detector is, in principle, a Michelson interferometer with multi-kilometer long Fabry Perot cavities in its arms. The mirrors of the interferometric gravitational wave detector are suspended as pendulums. In order to isolate the interferometer from the ground motion and align the mirrors relatively to each other, multi-stage isolation systems are used. For the next generation of the proposed American detector called Advanced LIGO, three cascading sub-systems have been developed [35] and are shown in Fig 1:

1. A hydraulic pre-isolator system (HEPI) for low frequency alignment and control, which will be situated outside the vacuum system.
2. A two-stage in-vacuum active isolation platform designed to give a factor of ~1000 attenuation at 10 Hz
3. A multiple pendulum suspension system (quadruple pendulum for the most sensitive optics and triple pendulum otherwise) that provides passive isolation above a few hertz, and minimizes suspension thermal noise by using high Q materials in the final stage.

The combination of these three sub-systems will reduce the displacement noise of the test mass of the pendulum to about $10^{-19}\ m/\sqrt{Hz}$ at 10Hz.

3.2 ADVANCED LIGO SUSPENSION, THE TRIPLE PENDULUM

The triple pendulum is the last stage of Advanced LIGO's seismic isolation. Its role is to filter the high (>10Hz) frequencies noise using 3 stages of passive isolation in the horizontal directions and 2 stages of isolation in the vertical direction. The pendulum is shown in Fig 2 and has been modeled and designed by Calum Torrie and Norna Robertson in Glasgow and Caltech [36]

The main purpose of the triple pendulum is to filter the high frequencies seismic noise and minimize the thermal noise. The thermal noise is calculated as a function of the structural dissipation thanks to the theorem of fluctuation-dissipation:

$$x_{therm}^2(\omega) = \frac{4k_b T\omega_0{}^2\alpha}{\omega\, m\left[\left(\omega_0{}^2 - \omega^2\right) + \omega_0{}^4\alpha^2\right]} \qquad \textit{Eq 3.1}$$

Where k_b is the Boltzmann's constant, T is the temperature and α is the structural internal dissipation. The lower the internal dissipation (the higher the Q factor), the lower the noise far from resonance. By building low dissipation suspensions, the noise off resonance will be lowered and resonances will be sharper and easier to filter.

Hence, the pendulum is made of low loss materials (fused silica wires), which also increases the Q of the low frequency rigid-body resonances. Unfortunately, this leads to a very large amplification of the seismic noise at those resonances.

Although these low frequencies aren't in the detection bandwidth of the LIGO interferometers, the resonances still need to be damped to keep the pendulum quiet enough so that the interferometers can perform.

An active control is used to damp the pendulum resonances. The first mass of the pendulum has six sensors/actuators that are used by the active control loop to damp the pendulum in the six degrees of freedom.

Using active control to damp the pendulum resonances also generates additional noise that needs to be accounted for. The electro-magnetic actuator noise is considered to be negligible at high frequencies; however, the sensor noise is relatively large as shown in the following section.

3.3 SEISMIC NOISE AND SENSOR NOISE

The two seismic isolation stages between the ground and the pendulum filter the seismic noise to a very low level. The anticipated seismic noise at the pendulum attachment point for Advanced LIGO is plotted in Fig 3.

At this level, the noise floor of the sensors used to actively damp the pendulum is large compared to the motion. This noise has already been measured in laboratory. Above 10Hz, the noise comes from shot noise. Shot noise is a type of noise that occurs when the finite number of particles that carry energy, such as the photons in the case of our optical sensor, is small enough to give rise to detectable statistical fluctuations in a measurement. Below 10Hz, the noise goes up and this phenomenon has not been understood yet.

As we can see on Fig 3, the sensor noise becomes the dominant noise above 0.8Hz and becomes about 500 times larger than the seismic noise coming from the ground at 10Hz. This is unusual in the active control field.

In the active damping loop, this sensor noise will be processed and re-injected at high frequencies; thus deteriorating the passive isolation of the pendulum. The challenge is to design a control loop that damps the resonances but keeps the sensor noise transmission as small as possible.

3.4 FEEDBACK USING COLLOCATED IRR FILTER

In a frequency domain approach, filters are designed to reduce the high frequencies feedback gain as much as possible. The gain is then adjusted to provide a 10 seconds settling time to an impulse excitation. Designing such a filter is a long and complicated process and provides poor performance. The example for the filter in the X direction is given in Fig 4 : the plant, filter and open loop are plotted. The impulse response of the closed loop with the active control on and off is then plotted in Fig 5.

The amplitude of displacement noise at the bottom mass is plotted in Fig 6 using the seismic and sensor noise inputs expected for Advanced LIGO. We see that the damping loop significantly increases the noise at high frequencies. Unfortunately, this filter is giving the best results we can expect from this method, which means that improving the performance will only be possible by changing the damping strategy.

In the following section, we will show that we can use more advanced control schemes by using our knowledge of the pendulum. In order to get more tuning freedom to optimize the loop, we will use independent modal control. The modal decomposition is a great tool to decouple the control design and we will see that it also helps to decrease the sensor noise transmission. The modal states will be obtained thanks to an observer; the lack of measurements will be compensated by our knowledge of the pendulum's model. The observer can also be used to reduce the sensor noise transmission.

4 CONTROL BACKGROUND

The following section recalls the background of the well-known control and observation techniques used in this paper.

4.1 INDEPENDENT MODAL CONTROL

The controller we use is an Independent Modal Control (IMC), it consists of working in the modal basis where the equation of the dynamics are decoupled. Each mode will then be controlled and tuned independently. The main advantage of this strategy is that each mode can be studied both for damping performances and sensor noise transmission. In general, lower modes will tend to have a bigger influence on damping while higher modes are the ones transmitting the more sensor noise.

The equation of motion in the real basis (M is the mass matrix, K is the stiffness matrix and x is the vector containing the real states) is:

$$M\ddot{x} + Kx = F \qquad \textit{Eq 4.1}$$

$$x = Xe^{i\omega t} \qquad \textit{Eq 4.2}$$

$$M^{-1}KX = X\omega^2 \qquad \textit{Eq 4.3}$$

We call ϕ the matrix formed by the eigenvectors X .

$$x = \phi.q \qquad \textit{Eq 4.4}$$

$$\phi^t M\phi\,\ddot{q} + \phi^t K\phi\; q = \phi^t F \qquad \textit{Eq 4.5}$$

The last equations are decoupled, we chose to control each modal state q independently; the feedback force applied to the plant is then a linear combination of the modal forces. The diagram of the modal control loop is shown in Fig 7.

4.2 MODAL OBSERVER

Modal control can only be used if the modal state is known. In the case of the triple pendulum, this is not trivial because only the position of the first mass is measured, which is not enough to know the full modal state. However, it is possible to rebuild the modal state by using an observer. It consists of a model of the structure running in parallel with the real plant whose outputs are compared to the measurable outputs of the plant. The difference is minimized by using a feedback loop.

There are different ways to optimize this feedback. Some method like robust control method H∞ or H_2 could be used. These methods are easy to adapt to poorly known systems. However, robust controls are optimized for the worst-case scenario; they are very efficient when the model of the plant is not well known, but the performances they provide are usually poor.

In the LIGO case, the robustness is not necessary but high performance needs to be achieved. The model of the suspension is very well known and this information can be used with optimal control methods. We will use MIMO modal estimator optimized using the Linear Quadratic method in this paper. The state-space discrete diagram of the modal observer is given in Fig 8. The goal is to optimize L_m.

The estimated modal state and estimated measurement are:

$$\hat{q}_{k+1} = A_m \hat{q}_k + B_m u + L_m \left(y_k - \hat{y}_k \right) \quad \textit{Eq 4.6}$$

$$\hat{y}_k = C_m \hat{q}_k \quad \textit{Eq 4.7}$$

The observation error is the difference between the modal state and the estimated modal state:

$$\delta_k = q_k - \hat{q}_k \quad \textit{Eq 4.8}$$

And the observer is described by the following equation

$$\delta_{k+1} = A_m{}^T \delta_k + C_m{}^T z_k \quad \textit{Eq 4.9}$$

$$\textit{With } z_k = -L_m{}^T \delta_k \quad \textit{Eq 4.10}$$

We perform the optimization using the LQ method with the following cost function:

$$J = \frac{1}{2}\sum_{k=0}^{N} \delta_k^T Q_1 \delta_k + z_k^T Q_2 z_k \qquad \textit{Eq 4.11}$$

Q_1 and Q_2 are weighting matrices determined by the designer. The feedback gain matrix L_m is then calculated to minimize the cost function. A good description for the resolution of the LQ optimization is given in [31].

5 OPTIMIZATION

5.1 DAMPING AND FILTERING DUALITY

Our goal is to optimize the control loop so that it provides good damping performance while keeping the sensor noise transmission as low as possible. Fig 9 shows a simplified diagram of the loop:

The real motion of the pendulum's mass can be written as a function of the 2 uncorrelated input noises: the seismic noise and the sensor noise:

$$x = TF_{seismic}.w \; + \; TF_{sensor}.v \qquad \textit{Eq 5.1}$$

The optimization consists of minimizing TF_{sensor} in high frequencies (above 10Hz), often referred as sensor noise transmission while damping the resonances of $TF_{seismic}$. The damping requirements for advanced LIGO suspensions haven't been set yet; we choose to set our requirements to a 10sec settling time from an impulse excitation. The settling time is defined as the time it takes for the amplitude of the oscillation to remain lower than 10% of the maximum value.

In the following section, we will describe how to optimize both the modal controller and the modal estimator.

5.2 INDEPENDENT MODAL CONTROL

The modal controller's optimization consists in balancing the contribution of the sensor noise transmitted by each independent modal controller.
To begin with, the feedback gain of each individual modal controller is arbitrarily set up so that each mode damps with a settling time of 10 seconds. Then, the sensor noise transmission

TF_{sensor} for each modal controller is plotted. Fig 10 shows an example for a system with 3 degrees of freedom:

As we see in the high frequencies (above 10Hz), the sensor noise is mostly transmitted by the 3rd modal controller. The control gain of this mode can be reduced, while the gain of the two other controllers can be increased without increasing the total sensor noise transmission as shown in Fig 11. Thanks to this tuning, the total sensor noise transmission has been reduced by several decibels. Because the lower modes carry the most energy, the result on the overall damping performance will also remain the same as shown on Fig 12.

5.3 MODAL OBSERVER

The next step is to optimize the observer, so that the sensor noise transmission is reduced without decreasing the damping performance. This is done by carefully balancing the weighting matrices of the cost function (Eq 4.11).

The weighting matrix Q_1 enables us to weigh how rapidly we want to observe each mode. The larger these terms, the faster the estimation will be, but the greater the sensor noise transmission. We make the choice to design Q_1 so that each mode gets the same weight of 1.

The weighting matrix Q_2 enables us to weigh the participation of each measurement in the estimator dynamics. If the weight is large; the sensor noise transmission will be reduced. If the gain is small, the measurement contribution will increase and more sensor noise will be transmitted. On Fig 13, we show this behavior by plotting the sensor noise transmission (transfer function from sensor noise to bottom mass) at 20Hz against Q_2 .

One can also plot the damping performance for different values of Q_2 using a given controller; the settling time is plotted against Q_2 in Fig 14

We see that the larger Q_2, the longer the settling time. This is due to the fact that a “penalty” to the estimator’s internal feedback term has been added in the cost function. When Q_2 increases, the estimator becomes slower, this leads to a reduction of the damping performance. By choosing the right compromise between damping and sensor noise transmission, we can choose the best value of Q_2.

If more than one measurement is made, Q_2 is not a single weight anymore and becomes a matrix where cross couplings between measurements need to be taken into account. For LIGO pendulums, we often have 2 measurements available (displacement and angle of the top mass), in these cases, we chose to write Q_2 as

$$Q_2 = R_1 \begin{bmatrix} R_2 & \\ & \dfrac{1}{R_2} \end{bmatrix} \qquad \textit{Eq 5.2}$$

This formulation shows 2 terms, R_1 weights the overall weight of Q_2 compared to Q_1 . R_2 weights one measurement relative to the other, which enables us to handle cross-coupling.

As we have done before, the damping performance can be plotted against R_1 for different values of R_2 in Fig 15.

Since cross couplings play an important role, they need to be taken into account. Sensor noise levels might also be different for the displacement and the angular measurements. Hence, we plot the final amplitude of the bottom mass motion due to each of the contributing sensor noises instead of the sensor noise transmission. An example is shown in Fig 16.

We see that the trend we have seen with the simple case still exists here, the greater R_1 is, the lower the sensor noise transmission. R_2 also plays a very important role here. This minimum is due to cross couplings and will be explained in the next section.

5.4 STABILITY-ROBUSTNESS

In order to study the stability of the loop, the equations of the controlled-observed system are written:

$$x_{k+1} = Ax_k - BK_m\hat{q} = Ax_k - BK_m\left(\phi x_k - \delta_k\right) \qquad \textit{Eq 5.3}$$

$$\delta_{k+1} = A_m\delta_k - LC_m\delta_k \qquad \textit{Eq 5.4}$$

$$\begin{Bmatrix} x_{k+1} \\ \delta_{k+1} \end{Bmatrix} = \begin{bmatrix} A - BK_m\phi & BK_m\phi \\ 0 & A_m - LC_m \end{bmatrix} \begin{Bmatrix} x_k \\ \delta_k \end{Bmatrix} \qquad \textit{Eq 5.5}$$

The characteristic equation can be written

$$\det\left[\lambda I - \left(A - BK_m\phi\right)\right].\det\left[\lambda I - \left(A_m - LC_m\right)\right] = 0 \qquad \textit{Eq 5.6}$$

The poles of the controlled-observed system consist of the combination of the estimator poles and the controller poles that are unchanged from those obtained assuming actual state feedback. Since we have designed both the modal controller and the estimator to be stable, the whole loop will also be. However, this principle named separation principle is not systematic.

If the model and the system don't match because of a parameter mismatch, the poles of the system will be different from the poles of the estimator and the controller alone. Such parameter mismatches can be simulated in our loop using a Monte-Carlo.

After randomly changing the parameters (wire length, weights, inertias…) in the plant simulation, the poles of the modified loop are computed and plotted on a real/imaginary axis. These random mismatches can be repeated a large number of tries. By counting the poles in the real positive plane, the number of unstable loops that have been generated can be estimated.

Fig 17 shows the example of the Monte-Carlo pole map if the parameter mismatches are between -20 and +20%. The unmodified loop poles are shown with white dots and poles from randomly changed loops are shown in black. The probability to get an unstable loop is 4.8% (+/- 2%).

This method allows us to be more confident of the robustness of the control. Large (>10%) parameter mismatches are necessary to turn the loop unstable. Fortunately, we don't expect any parameter mismatch to be greater than 5% for the triple pendulum.

6 APPLICATION TO ADVANCED-LIGO TRIPLE PENDULUM

In this section, we apply our control strategy to the X/Pitch direction of a triple pendulum. The plant has six resonance frequencies (see Table 1) that all need to be damped. Both the pitch angle and the X displacement of the first mass are measured, couplings between the 2 degrees of freedom is taken into account.

The sensor noise in pitch ($rad/\sqrt{Hz}$) contributes more than the one in the X direction ($m/\sqrt{Hz}$) because of the small lever arm between the sensors used to measure the pitch (6cm).

The modal controllers use a very simple filter to damp each mode independently, Each filter has a zero at 0Hz to gain phase and for AC coupling, and a complex pair of poles at twice the resonance frequency of the mode to filter the higher frequencies while keeping a safe phase margin.

The gain for each controller is optimized using the technique we have seen in section 5.2 to get the best compromise between damping and sensor noise transmission. The gains are chosen as shown in Table 1.

The impulse response for each mode and for the bottom mass is plotted in Fig 18:

The estimator is a MIMO modal estimator optimized using the technique described previously. The key to optimizing the estimator is to choose the weights of the cost function (Eq 4.11) to minimize the sensor noise transmission while keeping good damping performance.

We plot the displacement noise and angular noise at 20Hz due to the sensor noise as a function of R_2 for various values of R_1.

As we see on Fig 19, the bigger R_1 is, the less the sensor noise transmission to the bottom mass. We also see that the plots have a minima; this is the limit where cross coupling becomes more important than the direct transmission. To the left of the minima, the noise at the bottom mass is dominated by the pitch sensor noise; right of the minima, the noise is dominated by the X sensor noise.

We must also adjust the damping performance. The settling time to an impulse is plotted in Fig 20 for several values of R_2.

The R_2 parameter balances the estimation of both degrees of freedom, if its value is too high or too small; one DoF will have very good damping performance while the other won't. By studying the noise plots and the damping plots together, we choose a good compromise to get good damping on both degrees of freedom and a good sensor noise filtering:

$R_1 = 0.1$

$$R_2 = 10^{0.5} \approx 3$$

The damping performance meets the 10 seconds settling time criteria. We now plot the noise at the bottom mass and compare it to the classic filtering approach in Fig 21

We see that there is a factor of 100 reduction between the classic loop noise and the modal loop noise at 20Hz. The same improvement is obtained in pitch.

7 EXPERIMENTAL VALIDATION

7.1 INTRODUCTION

This last section explains the experimental validation of our method. Unfortunately, Advanced LIGO isolation systems are not yet available, and hence we are not yet able to reach the seismic noise level we expected for advanced LIGO yet (see Fig 3). However, we can increase the sensor noise by artificially injecting more noise in the sensor inputs. We can then study the transfer function between this noise and the displacement of the pendulum's bottom mass.

Measuring the bottom mass motion is not easy at high frequencies (>10Hz), several problems need to be solved.

The first problem is the sensitivity required to measure the signal. The pendulum response to sensor noise falls as $1/f^6$ at the bottom mass. Between 10Hz and 100Hz, the amplitude of the signal has fallen by one million.

The second issue is that displacement sensors only measure the relative distance between the frame and the masses. As the frequency increases, the filtering increases at the bottom mass and the frame's motion becomes larger than the pendulum motion. In this regime, we aren't measuring the pendulum motion anymore, but the frame itself.

There is no sensor that can measure an inertial displacement at such sensitivity without adding undesired weight on the pendulum. Hence a relative displacement measurement between a pseudo inertial reference and the test mass under study is performed. The reference is quieter than the test mass because the test mass is driven by the elevated sensor noise. The pseudo inertial reference is another triple pendulum. The measurement is done by positioning the two

triple pendulums face to face and measuring the distance between the bottom mass of the pendulums optically.

Measuring the distance between 2 mirrors can be achieved with an excellent sensitivity using interferometric techniques. The Fabry-Perot cavity is an attractive way to measure small displacements because it can directly measure the distance between 2 parallel mirrors. We use the well-established Pound-Drever-Hall [33] technique to lock the cavity to a stabilized laser and measure the length of the cavity with a very high sensitivity.

The measurement involves building up an optical field in a cavity formed between two mirrors mounted on triple pendulums as shown in Fig 22. The phase and amplitude of the optical field that is reflected off the resonant cavity strongly depends on the separation of the mirrors. As one of the mirror moves, the PDH technique detects this phase shift and gives us a very accurate measurement of the length between the 2 masses. A feedback force is applied to the second pendulum to keep this length constant and keep the cavity at resonance. By knowing the force applied on the second triple pendulum, we know how much the first triple pendulum moved. A good description of this method is given by Eric Black in [34].

Our goal is to measure the transmission between the sensor noise and the bottom mass of the pendulum. Below 5Hz, the measurement is done with the shadow sensors, the displacement that we try to measure is big enough and these sensors are easy to use and reliable. Above 5Hz, the optical cavity measurement is used.

7.2 EXPERIMENTAL RESULTS

We compare 2 different types of damping loop:

1. The “classic” filtering feedback, as seen in section 3.4
2. The modal damping and MIMO estimator, as seen in section 6

The measured and modeled transfer functions are plotted in Fig 23 for both type of damping loops.

The high frequencies data agrees very well, between 5Hz and 25Hz, the data are clean and match the model almost perfectly. This is a very good result; it verifies our noise model at high frequencies, which is the most important part for sensor noise transmission.
The low frequencies agree well for the classic feedback too. For the modal damping, the data are slightly different than the model at some frequencies (minima at 1.1 Hz and noise at 4Hz), this

difference is not very significant, and most likely due to some mismatch between the model and the real plant, or some cross coupling that is larger than expected.

An interesting observation has also been made using this experiment. The dynamic of the second pendulum that is used to keep the cavity locked is heavily modified by the locking feedback. The feedback loop on this pendulum acts like an “inertial” clamp that virtually turns the triple pendulum into a double pendulum when the cavity gets locked. More measurements and information will be given about this phenomenon in an upcoming paper.

8 CONCLUSION

This paper shows that modern control schemes can be applied to minimize the sensor noise injection induced by an active control loop. Well known techniques such as the Independent Modal Control and the LQ estimation have been recalled, adapted and optimized toward an unusual objective in the field of active control: providing acceptable damping performance while minimizing sensor noise transmission in the loop.

The method presented in this work has been applied to solve the control challenges related to Advanced LIGO suspensions. Because of the extremely high isolation provided by the previous seismic isolation systems, the sensor noise introduced by the pendulum’s sensors is not negligible and needs to be accounted for. If standard active control techniques were used, this sensor noise would be re-injected into the pendulum and increase the displacement noise.

Instead, an independent modal control has been designed. The gain of each controller has been balanced to reduce the sensor noise. The first modes have a large control gain while the highest modes which carry most of the sensor noise have a smaller control gain. In order to use the modal decomposition and increase the noise filtering, a MIMO modal estimator was developed. Tools have been designed to optimize the estimator and the modal control loop so that they can provide the required damping while re-injecting a minimum amount of sensor noise. The damping performance and the sensor noise filtering have been balanced using these tools. The stability of the loop has also been checked in case the numerical model and the plant are not identical.

The method has then been applied a triple suspension. Excellent results have been obtained in simulation; the sensor noise transmission has been reduced by a factor of about 100 compared to a classic control approach, while keeping the same damping performance.

The simulation has been validated by an experiment. A Fabry-Perot optical cavity has been formed between 2 identical triple pendulums. Displacements to the order of the angstrom were measured using the Pound-Drever-Hall locking and measurement technique.

This control loop method was specifically designed and studied for Advanced LIGO triple pendulum but it also concerns any well modeled system where the sensor noise injection due to the control loop is an issue. Most of the applications for this technique can be found in very sensitive instruments where the performance of the system are so great that the sensor noise becomes non-negligible when control loops are designed. It is especially useful in the field of gravitational waves detection such as LIGO or VIRGO where the mechanical isolation performances of the systems are extremely high.

In the future, this work will be extended to other LIGO suspensions such as the quadruple pendulum used for the main interferometer optics. More work can also be done to automatically build an adaptive estimator that fits to the plant to improve the performances and robustness of the loop in the case of parameter mismatches between the plant and the model.

Acknowledgements

LIGO was constructed by the California Institute of Technology and Massachusetts Institute of Technology with funding from the National Science Foundation and operates under cooperative agreement PHY-0107417. This paper has LIGO Document Number LIGO-P070055-00-Z.

[1] A Einstein, Die Grundlage der Algemeinen Relativitatstheorie, Annalen der Physik 49, (1916), 769

[2] B Barish and R Weiss, LIGO and the Detection of Gravitational Waves, Phys. Today, 52, (1999), 44-50

[3] J R Smith et al, Commissioning, characterization and operation of the dual-recycled GEO 600, Class. Quantum Grav., 21, (2004), S1737-S1745.

[4] K. Tsubono and the TAMA collaboration, TAMA Project, Proc. of Conference on Gravitational Wave Detection, Tokyo, eds. K. Tsubono, M. K. Fujimotot, K. Kuroda, Universal Academy Press Inc., Tokyo, (1997), 183-191.

[5] J.Y. Vinet et al, Proc. of Gravitation and Cosmology, ICGC-95 Conference, Astrophysics and Space Library, Kluwer Academic Publishers 211, (1997) , 89-93.

[6] T.T. Soong, G.F. Dargush, Passive Energy Dissipation In Structural Engineering, Wiley, New York (1990)

[7] B.C. Nakra, Vibration Control In Machines And Structures Using Viscoelastic Damping, Journal Of Sound And Vibration, (1998), Vol 211 No 3, 449-465.

[8] R. Skinner, W. Robinson , G. Mcverry, An Introduction To Seismic Isolation. Wiley, Chichester, (1993).

[9] J. Giaime, P. Saha, D. Shoemaker , L. Sievers , A Passive Vibration Isolation Stack For LIGO: Design, Modeling, And Testing, Review Of Scientific Instruments 67 (1): 208-214 Jan 1996

[10] L. Meirovitch, Dynamics And Control Of Structure, Wiley, New York, (1990)

[11] A. Preumont, Vibration Control Of Active Structures : An Introduction, Kluwer Academics, Dordrecht, 2nd Edition (2002)

[12] L.Gaudiller, J. Der Hagopian, Active Control Of Flexible Structures Using A Minimum Of Components, Journal Of Sound And Vibration, 193(3), P713-741. (1996)

[13] S. Kim , S. Elliott, M. Brennan, Decentralized Control For Multichannel Active Vibration Isolation, IEEE Transactions On Control Systems Technology 9 (1): 93-100 (2001)

[14] S.J. Richman, J. Giaime, D.B. Newell, R.T. Stebbins, P.L Bender , J.E. Faller, Multistage Active Vibration Isolation System, Review Of Scientific Instruments 69 (6): 2531-2538 (1998)

[15] D.Karnopp, Design Principles For Vibration Control Systems Using Semi-Active Dampers, Journal Of Dynamic Systems, Measurement, And Control 112 (1990), Pp. 448–455.

[16] D. Karnopp, Active And Semiactive Vibration Isolation, Journal Of Mechanical Design 117: 177-185 Sp. Iss. B, (1995)

[17] J. Der Hagopian, L. Gaudiller, B. Maillard, Hierachical Control Of Hydraulic Active Suspensions Of A Fast All-Terrain Military Vehicle, Journal Of Sound And Vibration, 222(5), P723-752. (1999)

[18] M.D. Symans, M.C. Constantinou, Semi-Active Control Systems For Seismic Protection Of Structures: A State-Of-The-Art Review, Engineering Structures, Volume 21, Issue 6 ,(1999), Pages 469-487

[19] P Fritschel, Second generation instruments for the Laser Interferometer Gravitational Wave Observatory (LIGO), Gravitational-Wave Detection, M. Cruise, P. Saulson Eds. 4856, 282-291, SPIE, Bellingham, WA. (2003)

[20] R Abbott, R Adhikari, G Allen, S Cowley, E Daw, D DeBra, J Giaime, G Hammond, M Hammond, C Hardham, J How, W Hua, W Johnson, B Lantz, K Mason, R Mittleman, J Nichol, S Richman, J Rollins, D Shoemaker, G Stapfer and R Stebbins, Seismic isolation for Advanced LIGO, Class. Quantum Grav. 19, (2002), 1591-1597

[21] N.A Robertson and LIGO collaboration, Seismic isolation and suspension systems for Advanced, Gravitational Wave and Particle Astrophysics Detectors, SPIE, vol. 5500, ed. James Hough, Gary Sanders, (2004), 81-91

[22] S. Aston, C. Speake, Geometric OSEM Sensor development, LIGO document, T040043-01-K, (2004)

[23] K. Ogata, Modern Control Engineering, Prentice Hall, (2001)

[24] C.R Fuller, S.J Elliot, P.A Nelson, Active control of Vibration, Academic Press, New York, (1997)

[25] S. Aston, C. Speake, Interferometric OSEM Sensor development, LIGO document, T040044-01-K, (2004)

[26] K. A. Strain, M. V. Plissi, C. I. Torrie, M. Barton, N. A. Robertson, A. Grant, C. A. Cantley, P. A. Willems, J. H. Romie, K. D. Skeldon, M. M. Perreur-Lloyd, R. A. Jones, J. Hough, An investigation of eddy-current damping of multi-stage pendulum suspensions for use in interferometric gravitational wave detectors, Review of scientific instruments, Volume 75, number 11, (2004)

[27] G.Losurdo, D.Passuello, Noisy sensors in control loops: an idea to reduce re-injected noise (part I). VIRGO document, VIR-NOT-FIR-1390-256, (2003)

[28] W.K Gawronski, Dynamics and control of structures: A modal approach, Springer, New York, (1998)

[29] A. Baz, S. Poh, J. Fedor, Independent modal space control with positive position feedback. ASME 14, (1992), 96-103.

[30] D. G. Luenberger, Observers for Multivariable Systems, IEEE Transactions on Automatic Control, AC–11:2 (1966), 190-197.

[31] G.F. Franklin, J.D. Powell, M Workman, Digital control of dynamic systems, Addison Wesley, (1990)

[32] R.E. Kalman, A new approach to linear filtering and prediction problems, ASME, journal of Basic Engineering, 82 (series D), (1960)

[33] R.W.P Drever et al., Laser Phase and Frequency Stabilization Using an Optical Resonator, Applied Physics B 31, 97 (1983)

[34] E. D. Black, An introduction to Pound-Drever-Hall laser frequency stabilization, American Journal of Physics, Volume 69, Issue 1, (2001), 79-87.

[35] N.A Robertson and LIGO collaboration, Seismic isolation and suspension systems for Advanced, Gravitational Wave and Particle Astrophysics Detectors, SPIE, vol. 5500, ed. James Hough, Gary Sanders, (2004), 81-91

[36] Calum I.E Torrie, Development of the suspensions for the GEO 600 gravitational wave detector, University of Glasgow, (2000)

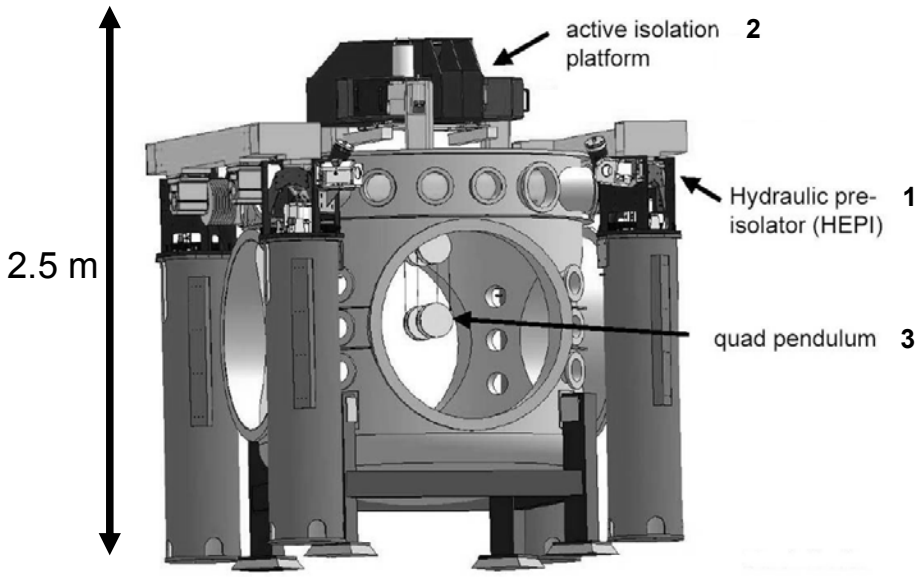

Fig 1: LIGO seismic isolation sub-systems

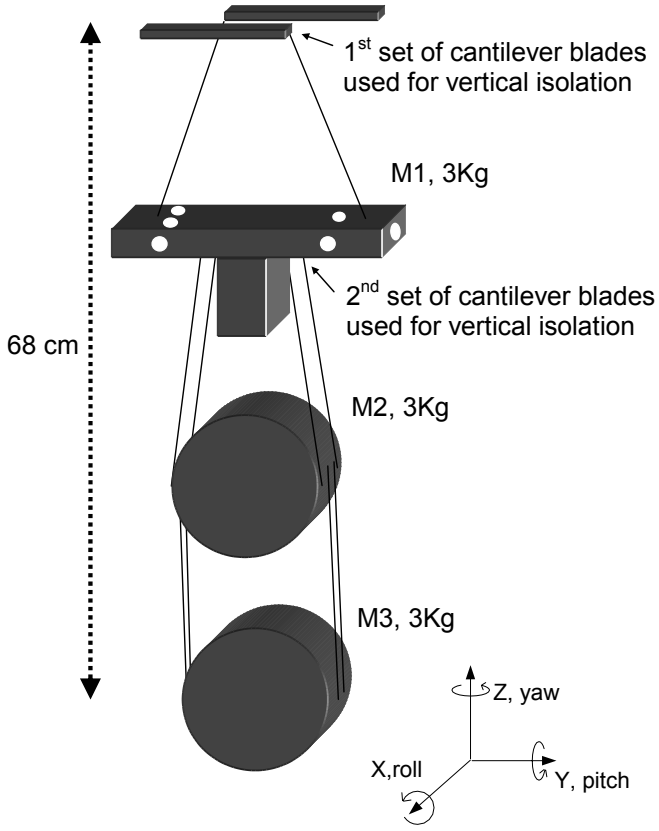

Fig 2: triple pendulum

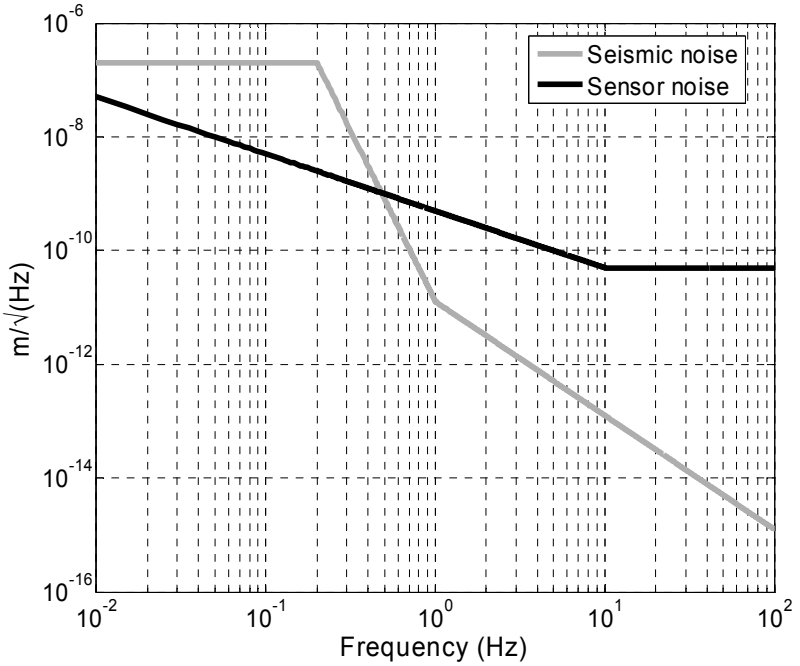

Fig 3: Amplitude of the seismic noise and sensor noise

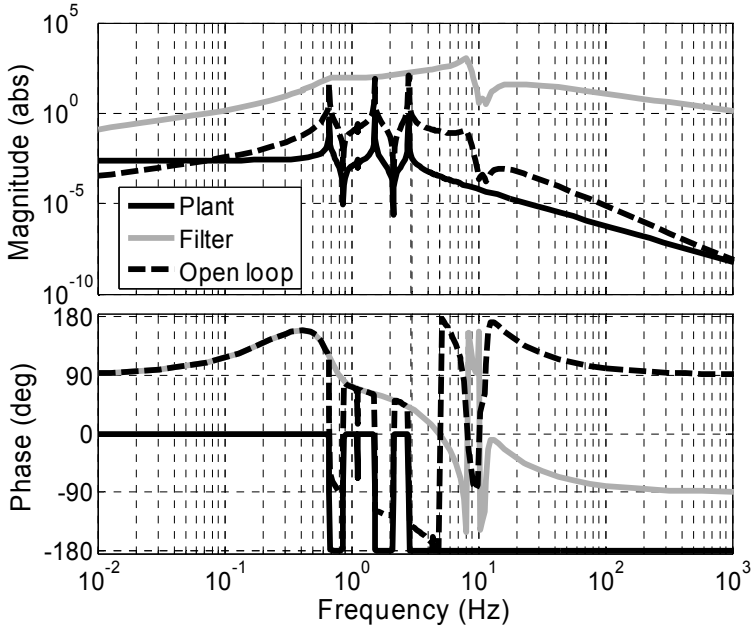

Fig 4: Loop plant and filter for classic control

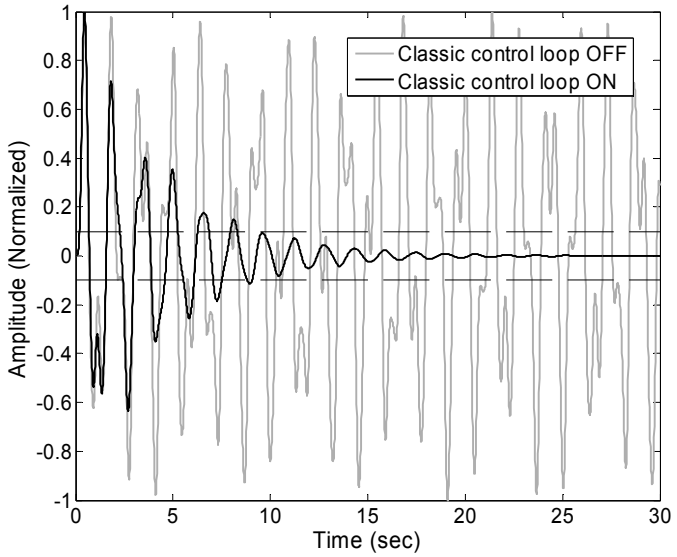

Fig 5: Impulse response with classic control on/off

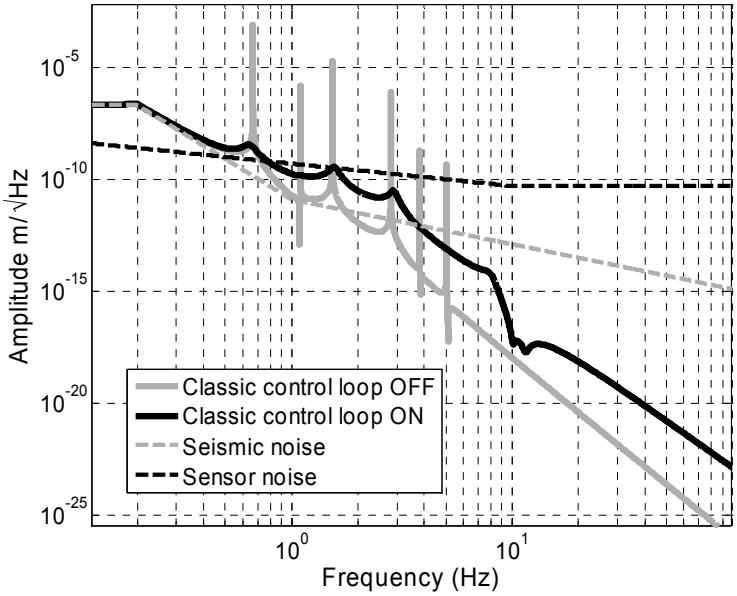

Fig 6 : Displacement noise at the bottom mass with classic control on/off

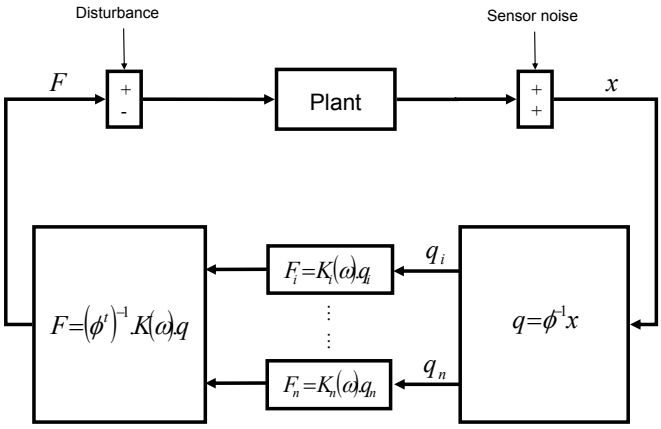

Fig 7: Modal control

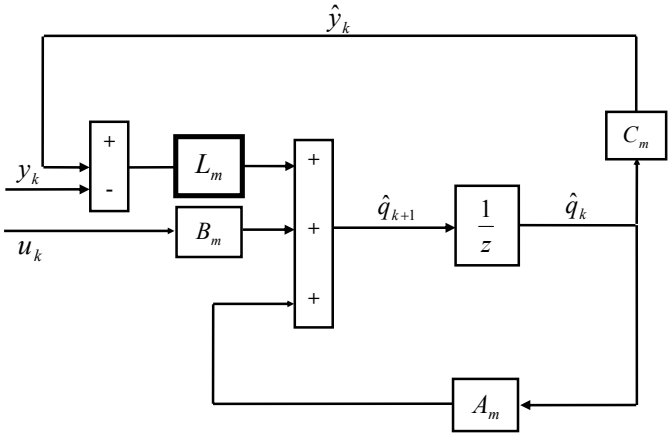

Fig 8: Prediction discrete estimator

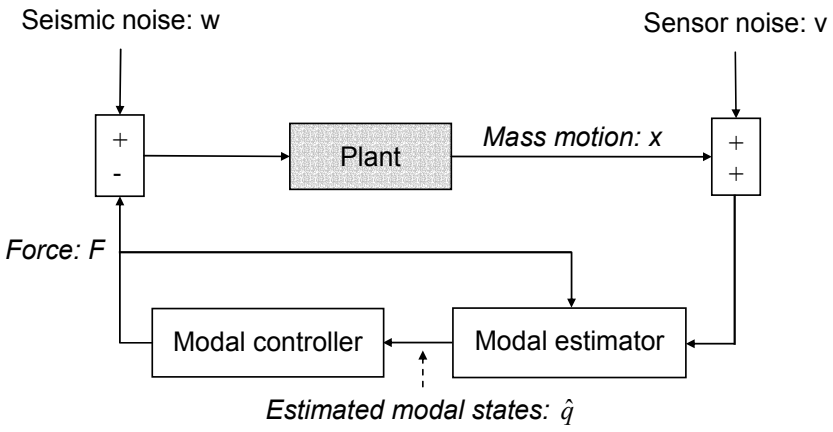

Fig 9: Simplified diagram of the loop

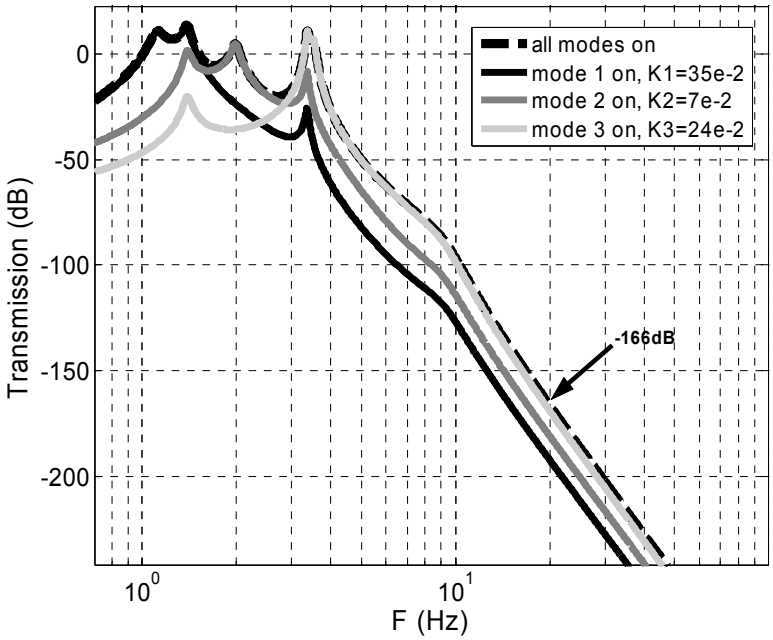

Fig 10: Sensor noise to bottom mass transmission with each modal controller on, non optimized

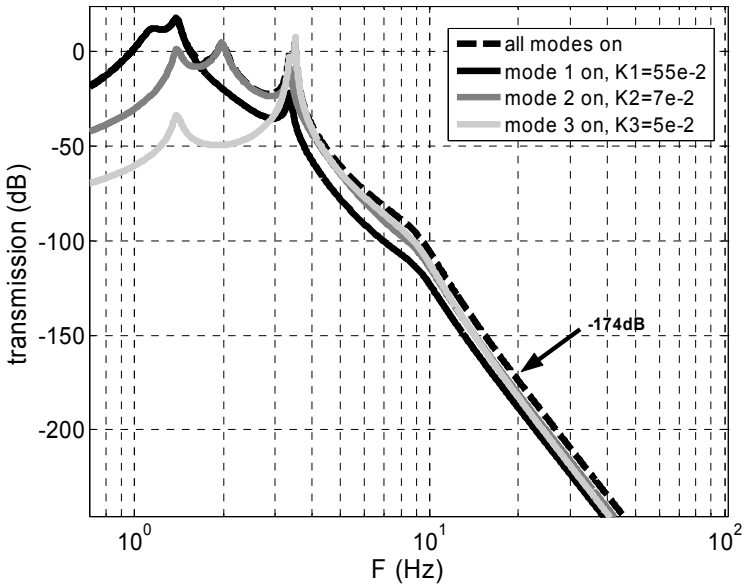

Fig 11: Sensor noise to bottom mass transmission with each modal controller on, optimized

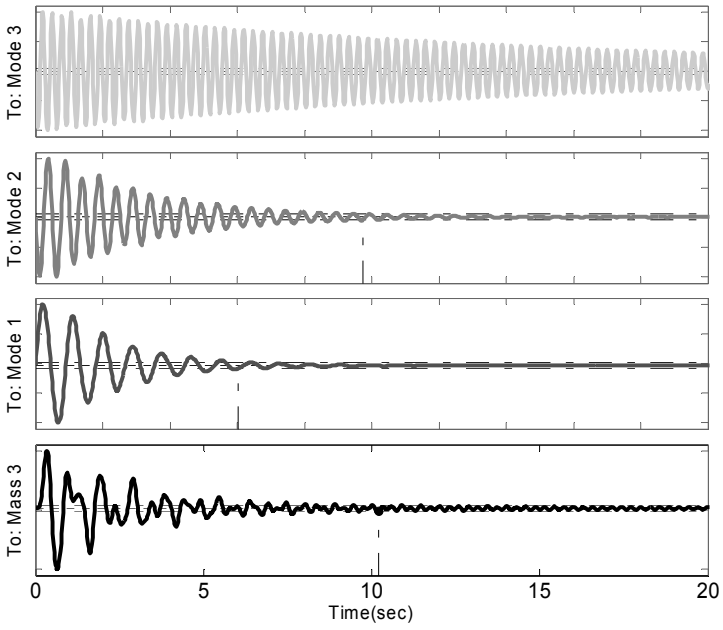

Fig 12: Modal and physical response to an impulse excitation

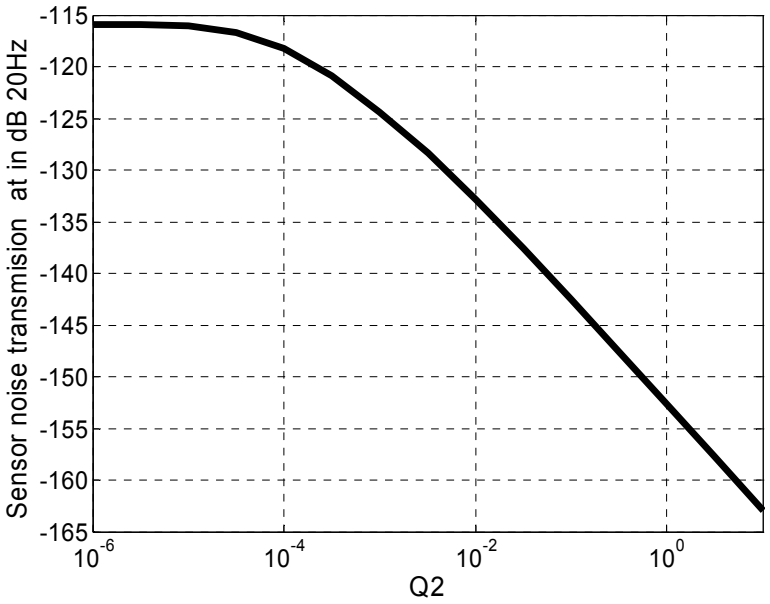

Fig 13: Sensor noise transmission against Q2

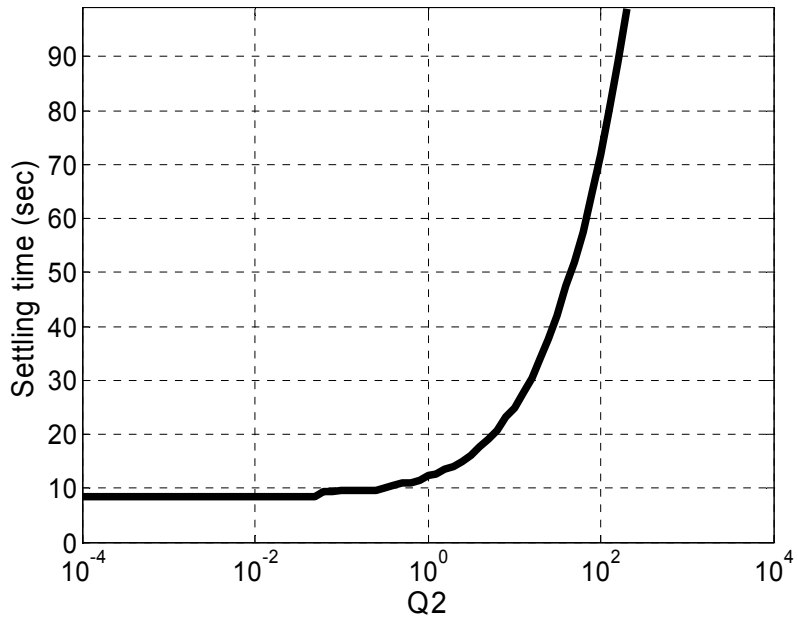

Fig 14: Damping performances against Q2

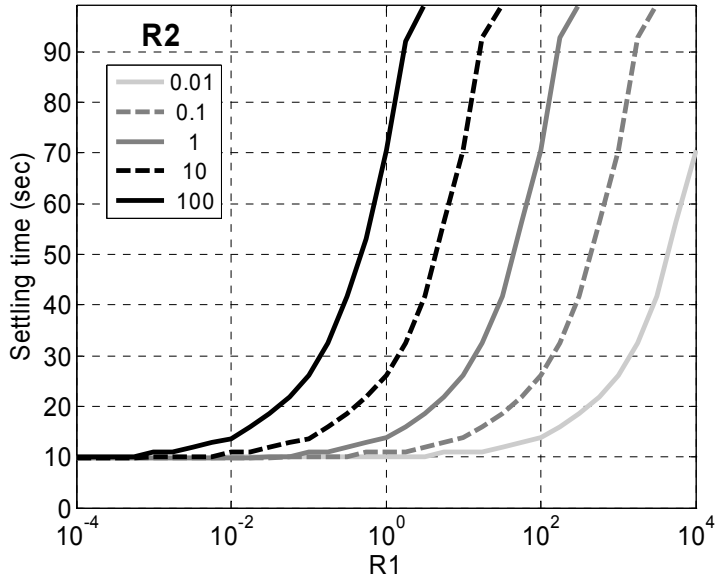

Fig 15: Damping performances against R1 for different values of R2

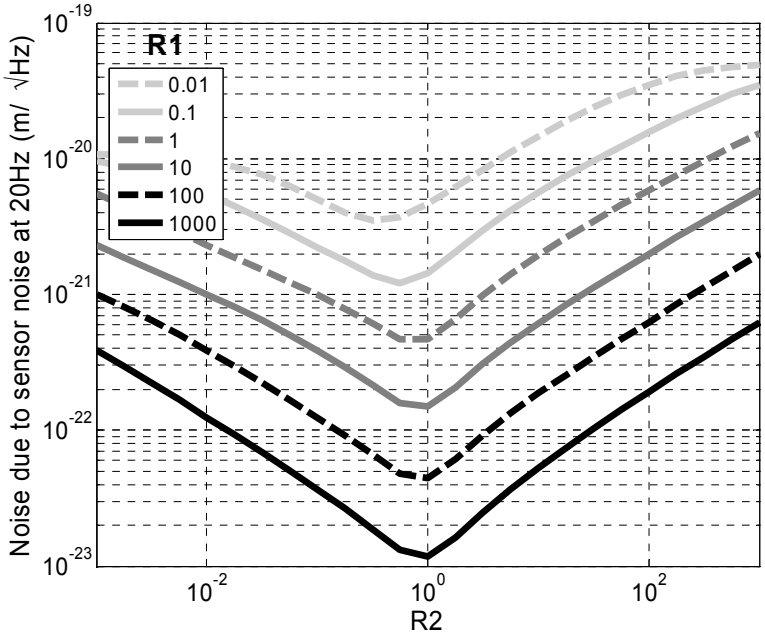

Fig 16: Noise due to sensor noise at 20Hz against R2 for different values of R1

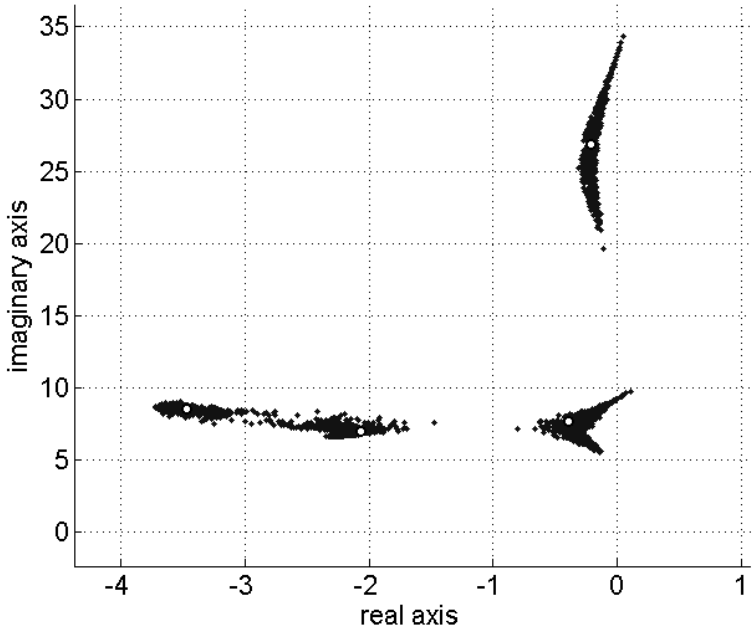

Fig 17: pole map with model mismatch (+/- 20%)

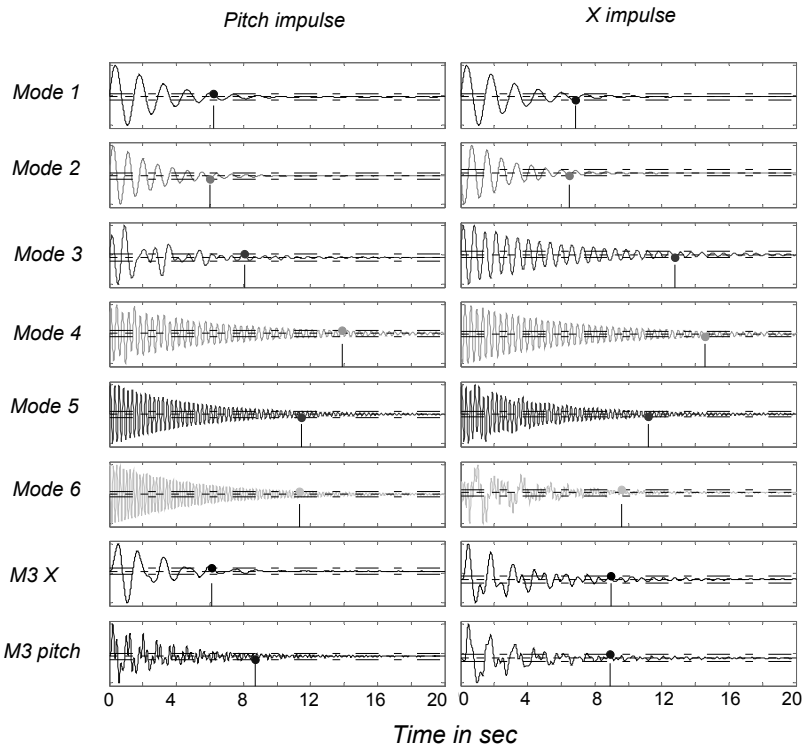

Fig 18: Modal and physical response to an impulse excitation, X and pitch

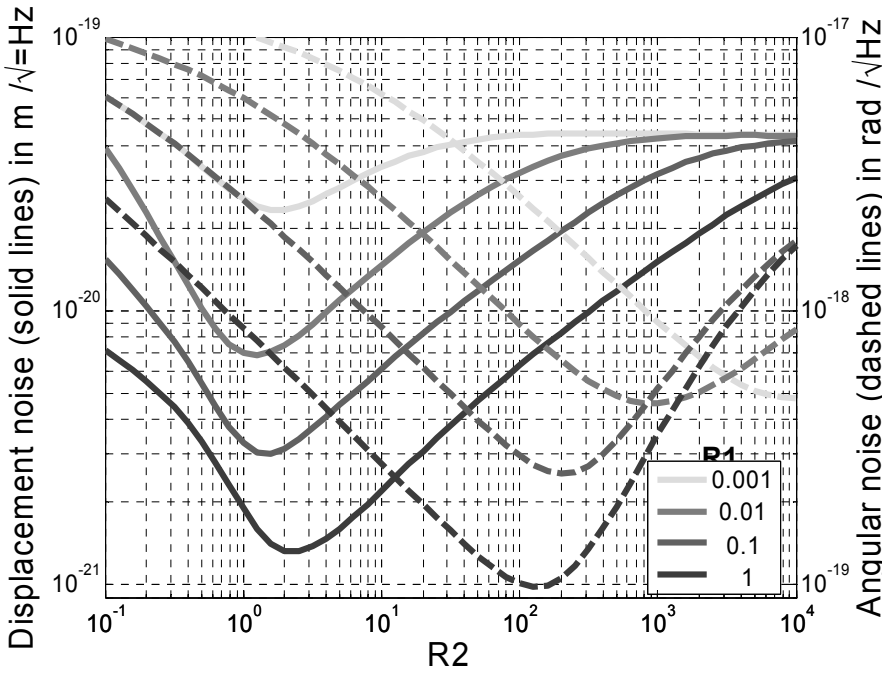

Fig 19: Amplitude of noise due to sensor noise at the bottom mass, X and pitch

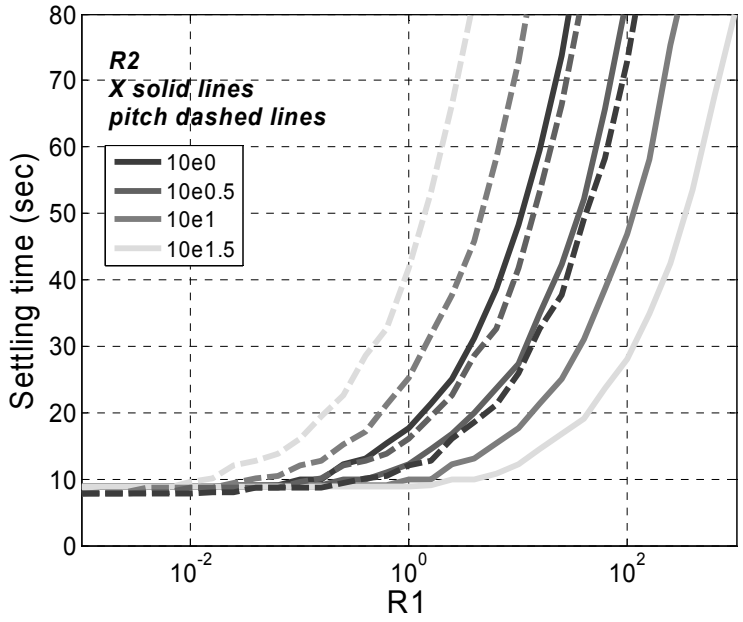

Fig 20: Settling time for X and pitch against R1 for different values of R2

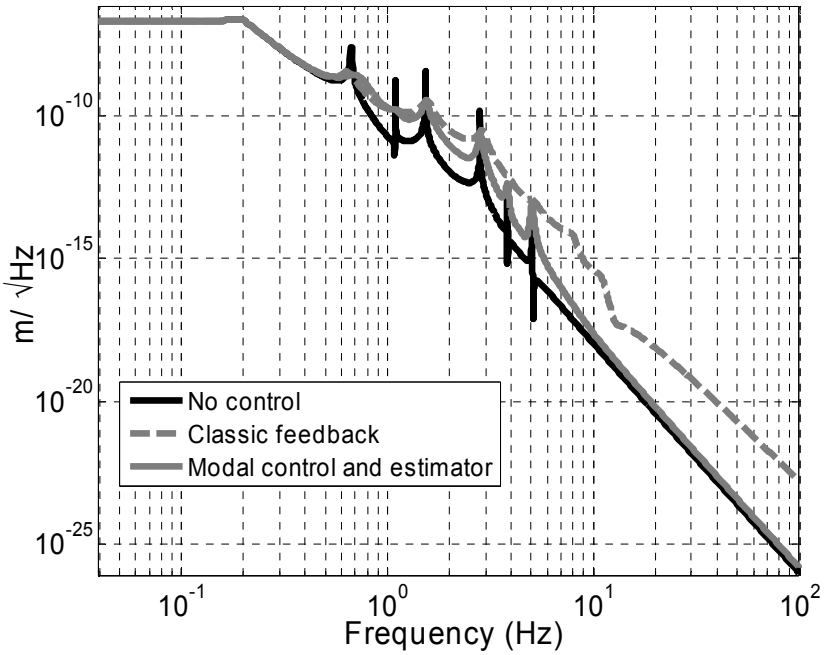

Fig 21: Displacement noise at the bottom mass in the X direction

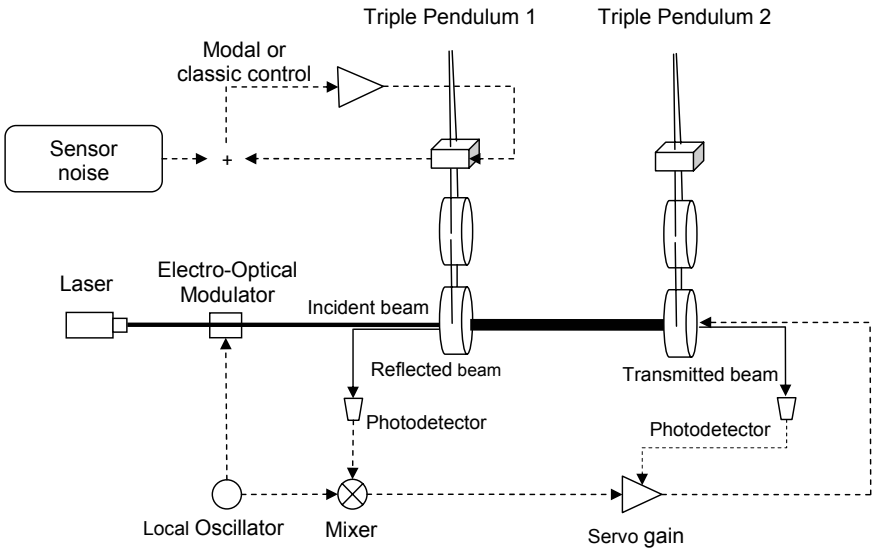

Fig 22: Optical cavity experiment layout

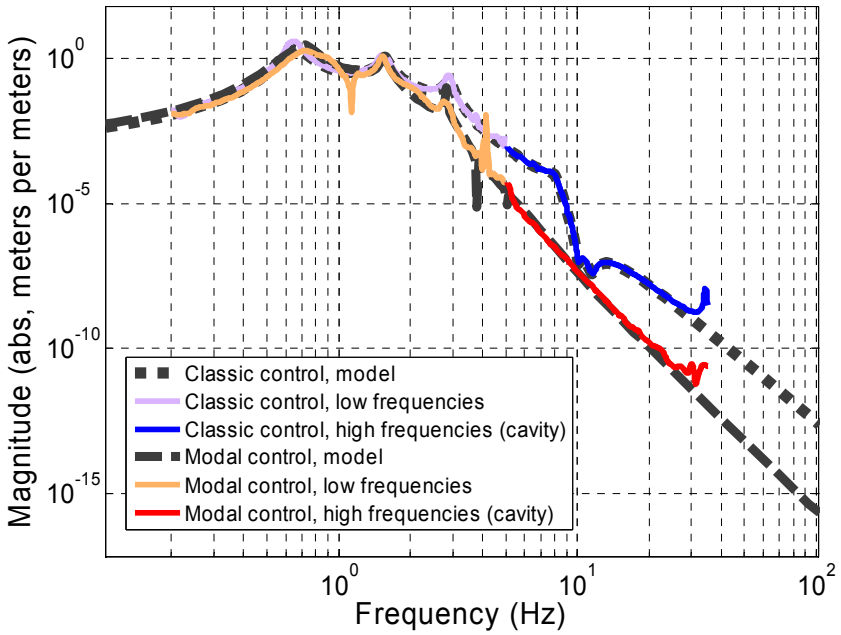

Fig 23: Transfer function between sensor noise and Mass 3 in the X direction, using 2 different control strategies

Mode	Type	Frequency (Hz)	Feedback gain K
1 :	X mode	0.65	50
2 :	Pitch mode	1.15	2
3 :	X mode	1.5	20
4 :	X mode	2.8	1
5 :	Pitch mode	4.1	8e-3
6 :	Pitch mode	5.7	2e-3

Table 1: X /pitch resonances and modal controller gains